Project Report
LSP-289

High-Rate Entanglement Swapping with Spectrally Pure Photons: FY19 Quantum System Sciences Line-Supported Program

C. Lee
R.P. Murphy
M.E. Grein
P.B. Dixon

2 March 2020

Lincoln Laboratory
MASSACHUSETTS INSTITUTE OF TECHNOLOGY
LEXINGTON, MASSACHUSETTS

This report is the result of studies performed at Lincoln Laboratory, a federally funded research and development center operated by Massachusetts Institute of Technology. This material is based upon work supported by the Under Secretary of Defense for Research and Engineering under Air Force Contract No. FA8702-15-D-0001. Any opinions, findings, conclusions or recommendations expressed in this material are those of the author(s) and do not necessarily reflect the views of the Under Secretary of Defense for Research and Engineering.

Massachusetts Institute of Technology
Lincoln Laboratory

High-Rate Entanglement Swapping with Spectrally Pure Photons: FY19 Quantum System Sciences Line-Supported Program

C. Lee
R.P. Murphy
M.E. Grein
P.B. Dixon

Group 67

Project Report LSP-289

2 March 2020

Lexington Massachusetts

This page intentionally left blank.

TABLE OF CONTENTS

This page intentionally left blank.

LIST OF FIGURES

This page intentionally left blank.

1. INTRODUCTION

Quantum networks enable new and more powerful applications with performance above that which could be obtained classically [1,2]. Entanglement is the resource underlying the performance advantages of quantum networks: It is required for the teleportation of arbitrary quantum states [3], such as the inputs or outputs of a quantum computation, and it also provides stronger-than-classical correlations between remote elements, such as distributed networks of quantum processors [4], clocks [5], or sensors [6,7].

To achieve the performance gains of a quantum network, entanglement must be distributed between multiple network nodes. The required rate and range of entanglement distribution are application-dependent, but useful rates and distances remain beyond the reach of today's technology. Longer distances lead to lower rates because channel loss scales with distance. Entanglement swapping is a method for increasing the distance between remote entangled nodes while maintaining usable rates. Since the first laboratory demonstration of entanglement swapping [8], there have been many successive developments toward entanglement swapping for quantum networking, including entanglement swapping between fully independent sources [9,10] and entanglement swapping in a fiber network testbed [11].

Entanglement swapping works best with entanglement sources that produce photons in spectrally pure states. Spectrally pure photons are required for high-visibility Hong-Ou-Mandel (HOM) quantum interactions [12], including the Bell state measurement (BSM) that underlies entanglement swapping. The spectral purity of the input photons places an upper bound on the fidelity of the output swapped state; thus, entanglement swapping with spectrally pure states is necessary to ensure high-quality, long-distance entanglement distribution for quantum network applications.

The most commonly used sources of entangled photons are based on spontaneous parametric downconversion (SPDC) in nonlinear optical crystals, such as periodically poled potassium titanyl phosphate (PPKTP). Spectrally pure photons can be obtained from SPDC sources based on PPKTP by selectively engineering the pump and crystal properties. For example, in what are called the group-velocity-matching (GVM) conditions, if the pump, signal, and idler wavelengths are chosen such that the photons have zero group-velocity mismatch and the pump bandwidth is also matched to the crystal phase-matching bandwidth, then the signal and idler photons are output in a spectrally pure biphoton state [13]. The spectral purity can be further enhanced by modifying the periodic poling grating structure to alter the crystal phase-matching function [14].

Entanglement swapping has been demonstrated using sources designed for spectral purity under the GVM conditions, with a spectral purity of 82% [15]. Sources designed with custom poling have been used to demonstrate high-visibility HOM interference between photons produced by successive pump pulses [16] and by separate crystals [17]. Here we report a demonstration of entanglement swapping between two sources optimized for high spectral purity, using both the GVM conditions and a custom poling profile. Our demonstration also included a passive temporal multiplexing scheme that increased the entanglement generation rate while maintaining a high signal-to-noise ratio.

This page intentionally left blank.

2. HIGH-RATE SOURCES OF SPECTRALLY PURE POLARIZATION-ENTANGLED PHOTONS

We built two identical entanglement sources based on SPDC in bulk PPKTP crystals. The two sources were pumped by a single shared laser. The laser was a mode-locked titanium sapphire laser (Spectra Physics Tsunami) emitting picosecond pulses at a fundamental repetition rate of 80 MHz. To increase the system clock rate, we built a passive temporal multiplexer that used delay-line interferometers (DLIs) to split and recombine each pulse with a temporal offset between the two components. By using up to four DLIs in series, we could multiply the system clock rate by up to 16x, for a maximum rate of 1.28 GHz. In practice, the pump laser output was average-power-limited, so each successive multiplier stage doubled the repetition rate and halved the power per pulse. This passive temporal multiplexing scheme is commonly used to improve the signal-to-noise ratio (SNR) in experiments based on SPDC sources [18, 19]. For a single SPDC source, the probability of undesired multi-pair emissions is reduced while the desired twofold coincidence rate remains constant. For multiple SPDC sources, the probability of undesired coincidences due to multi-pair emissions decreases more quickly than the desired coincidence rate between photons produced by independent sources; that is, in our average-power-limited scenario, each successive multiplier stage increases the SNR but also reduces the desired coincidence rate. We determined that our optimal operating point, maintaining a trade-off between SNR and coincidence rates, was 4x multiplication, or a 320 MHz system clock rate.

We obtained spectrally pure SPDC photons by operating under the GVM conditions combined with a Gaussian phase-matching function. The pump was centered at 791 nm, and the signal and idler were both around 1582 nm. The Gaussian phase-matching function was obtained by modulating the duty cycle of each poling period along the length of the PPKTP crystal [14].

We first characterized the spectral purity of each individual SPDC source by measuring the joint spectral intensity (JSI) of the signal-idler pairs. We pumped the sources with 0.6 nm of bandwidth and used dispersion-based spectroscopy to convert spectral information to timing information [20] and timed the coincident photon detections with respect to a reference signal derived from the pump laser. The JSI is plotted in Fig. 1 and indicates 96% spectral purity.

The two-source quantum interference visibility, measured in a heralded HOM interference experiment, provides another, more complete indicator of spectral purity. We measured HOM interference between the two signal photons from the two sources, using the detections of the idler photons to herald the presence of the respective signal photons. The heralded HOM interference is plotted in Fig. 2, which shows a visibility of $(91 \pm 3)\%$.

We generated polarization-entangled photon pairs using the "beam-displacer" method [21–23], in which the PPKTP crystal is embedded within a compact Mach-Zehnder interferometer. The small spatial extent of the interferometer allows its alignment, and thus the polarization state quality, to remain stable, allowing the source to operate for several days at a time without requiring adjustment.

Our entangled-photon sources produced states of the form $|\psi\rangle = \alpha|HH\rangle_{1,2} + \beta e^{i\phi}|VV\rangle_{1,2}$, where the subscripts 1 and 2 indicate Photons 1 and 2, and $\sqrt{|\alpha|^2 + |\beta|^2} = 1$. The relative

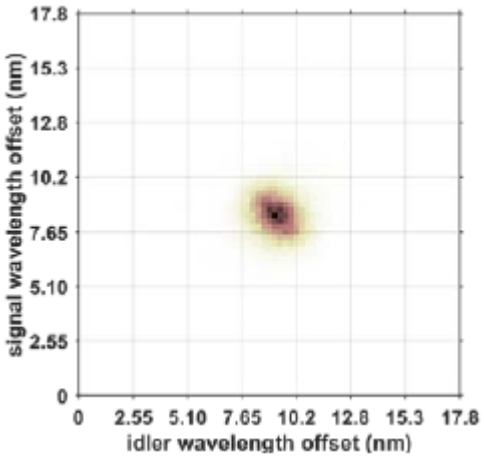

Figure 1. Joint spectral intensity for biphoton state produced by spectrally pure SPDC source. Axis units represent the offset from a reference wavelength; the absolute wavelength value is less important than the scales of the two axes.

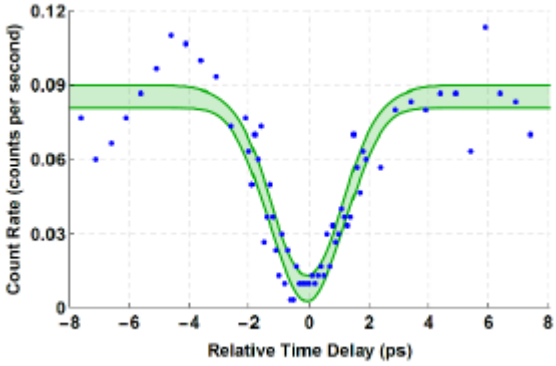

Figure 2. Heralded HOM interference between the signal photons produced by independent SPDC sources. The green band indicates the 95% confidence interval of the Gaussian fit.

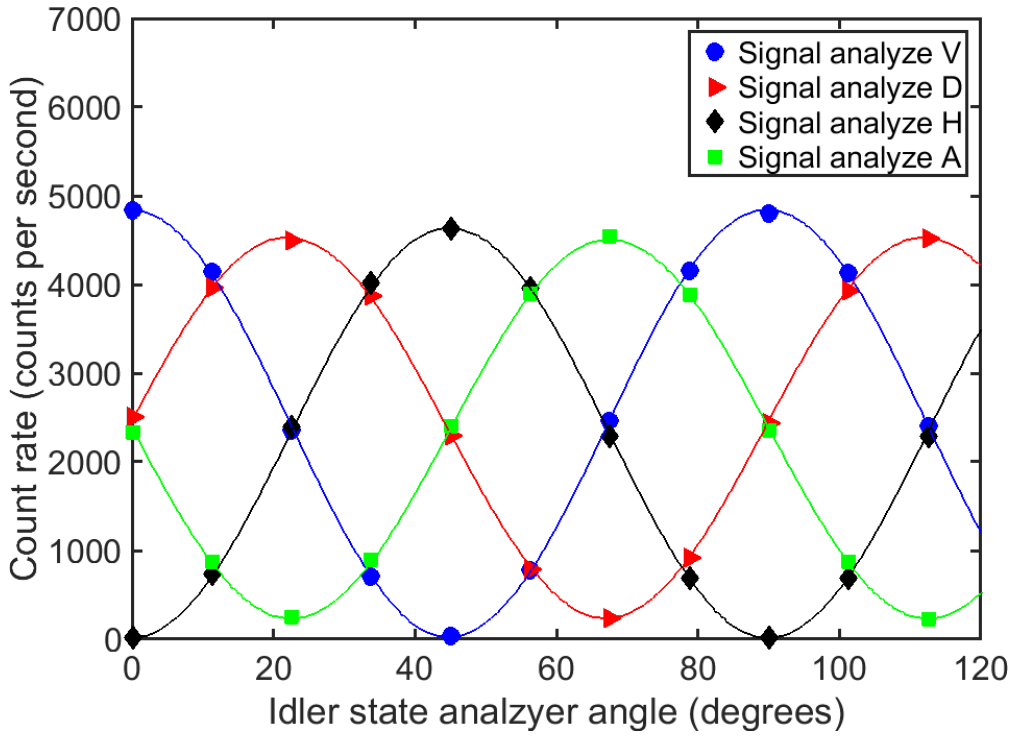

Figure 3. Polarization correlations between photon pairs produced by Source 1. H/V basis visibility: 99.0%. D/A basis visibility: 90.0%.

magnitudes of α and β were controlled by the pump polarization, and the phase ϕ was set by the angle of the pump beam displacer. We set the pump polarization and BD1 of each source to produce the maximally entangled Bell state $|\phi^+\rangle = \frac{1}{\sqrt{2}}(|HH\rangle_{1,2} + |VV\rangle_{1,2})$. The polarization of each photon was measured using an analyzer comprising a quarter-wave plate (QWP), a half-wave plate (HWP), and a linear polarizer. These three elements allowed the projection of the photon polarization onto any basis state, such as horizontal (H), vertical (V), diagonal (D), or antidiagonal (A). These basis states are relevant for analyzing the entangled state quality.

The quality of the entangled state was assessed by counting coincidences between Photons 1 and 2 for certain settings of their respective polarization analyzers. For example, the polarization correlations were measured by holding the signal analyzer at a fixed setting and sweeping the angle of the idler analyzer's HWP. These data are shown in Fig. 3. In the H/V basis, the visibility was 99.0%, and in the D/A basis, the visbility was 90.0%. The lower visibility in the D/A basis is due to alignment imperfections in the entanglement source setup; specifically, there is unwanted spatial overlap between the two arms of the compact Mach-Zehnder interferometer. We believe that this can be corrected in the near future by increasing the spatial extent of the interferometer.

This page intentionally left blank.

3. POLARIZATION ENTANGLEMENT SWAPPING

Using two entanglement sources producing the $|\phi^+\rangle$ Bell state, entanglement swapping is mathematically described as

$$|\phi^+\rangle_{1,2} \otimes |\phi^+\rangle_{3,4} = \frac{1}{2}\left(|HH\rangle_{1,2} + |VV\rangle_{1,2}\right) \otimes |HH\rangle_{3,4} + |VV\rangle_{3,4}) \quad (1)$$

$$= \frac{1}{2}\left(|\phi^+\rangle_{1,4} \otimes |\phi^+\rangle_{2,3} + |\phi^-\rangle_{1,4} \otimes |\phi^-\rangle_{2,3} + |\psi^+\rangle_{1,4} \otimes |\psi^+\rangle_{2,3} + |\psi^-\rangle_{1,4} \otimes |\psi^-\rangle_{2,3}\right) \quad (2)$$

where subscripts 1 and 2 (3 and 4) correspond to the photons produced by Source 1 (2). Photons 2 and 3 are sent to the Bell state measurement (BSM), and if the BSM is successful, then Photons 1 and 4 should be entangled. Using a partial BSM, we postselected events corresponding to the last term on the right-hand-side of Eq. (2), projecting Photons 1 and 4 onto the Bell state $|\psi^-\rangle = \frac{1}{\sqrt{2}}\left(|HV\rangle_{1,4} - |VH\rangle_{1,4}\right)$. We characterized the resulting entanglement between Photons 1 and 4 by measuring the polarization correlations between them, holding Photon 1's analyzer at a fixed setting and sweeping the angle of Photon 4's analyzer's HWP. These data are plotted in Fig. 4. In the H/V basis, the visibility was 94.7%, and in the D/A basis, the visbility was 55.1%. The fact that all the visibilities were above 33% indicates that Photons 1 and 4 are entangled, according to the Peres criterion for nonseparability [24]. This demonstrates entanglement swapping.

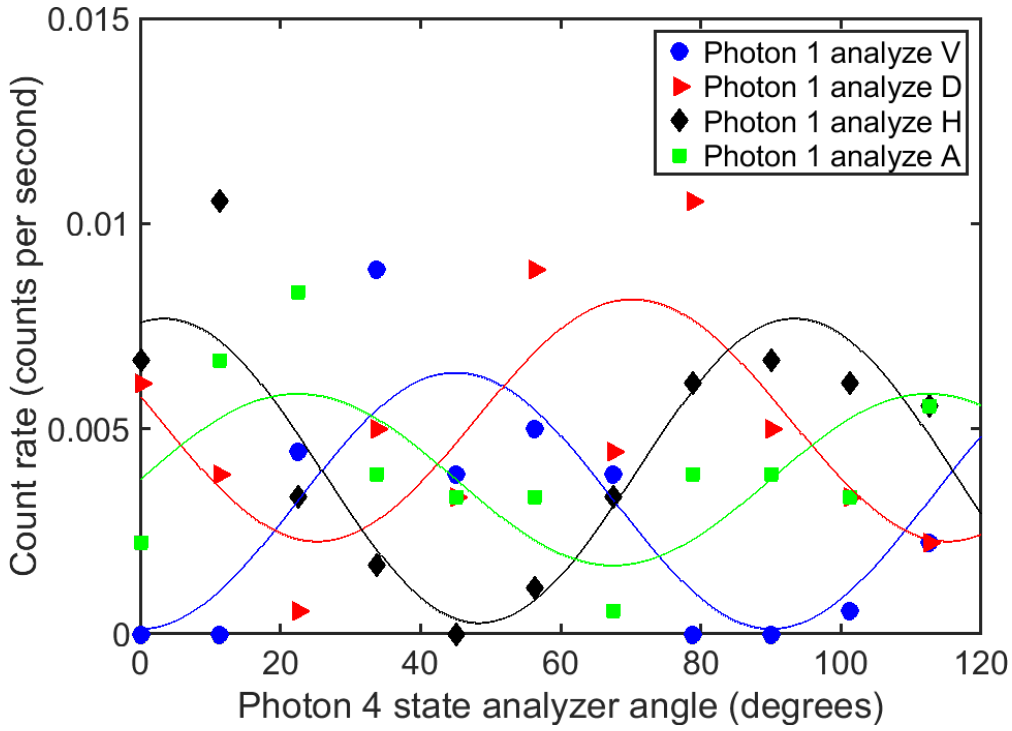

Figure 4. Polarization correlations between Photons 1 and 4 after entanglement swapping. Photon 1 = Idler 1. Photon 4 = Idler 2. H/V basis visibility: 94.7%. D/A basis visibility: 55.1%.

4. DISCUSSION AND FURTHER WORK

Here we have reported preliminary results for entanglement swapping between two entanglement sources that were optimized for high spectral purity. After the swap, the resulting polarization coincidence visibilities indicate that the output state of Photons 1 and 4 is nonseparable, i.e., entangled.

However, the output state is not Bell nonlocal, meaning that it would not pass a Bell inequality test [25] or be useful for high-fidelity quantum teleportation. It is clear that our entanglement swap demonstration can be improved. The high-visibility two-source HOM interference indicates that our spectral purity optimization worked and that spectral correlations between photons were not the limiting factor in our demonstration. The aspect that needs improvement is the quality of the entangled states produced by each entanglement source. The 90% D/A basis visibility is low enough to be cause for concern about the entangled state quality; it suggests that the two arms of entanglement-generating interferometer are experiencing some unwanted spatial overlap. We have identified and are currently working on an optical re-alignment method to remove this overlap, which we expect will improve the quality of each individual source's entangled state and of the entanglement swap demonstration as a whole.

We are also developing a free-space optical (FSO) testbed for entanglement swapping over a high-loss atmospheric channel. The primary goal of this effort is to test architectures for synchronizing the arrival of the two signal photons at the BSM after one photon has traveled over a long and possibly time-varying channel. The FSO testbed effort will lay the groundwork toward entanglement swapping between ground and orbiting platforms, expanding the physical reach of quantum networks with exciting possibilities for a new and wider application space.

This page intentionally left blank.

REFERENCES

[1] H.J. Kimble, "The quantum internet," *Nature (London)* 453(7198), 1023–1030 (2008).

[2] S. Wehner, D. Elkouss, and R. Hanson, "Quantum internet: A vision for the road ahead," *Science* 362, eaam9288 (2018).

[3] C.H. Bennett, G. Brassard, C. Crépeau, R. Jozsa, A. Peres, and W.K. Wootters, "Teleporting an unknown quantum state via dual classical and Einstein-Podolsky-Rosen channels," *Phys. Rev. Lett.* 70, 1895–1899 (1993), URL http://link.aps.org/doi/10.1103/PhysRevLett.70.1895.

[4] C. Monroe, R. Raussendorf, A. Ruthven, K.R. Brown, P. Maunz, L.M. Duan, and J. Kim, "Large-scale modular quantum-computer architecture with atomic memory and photonic interconnects," *Phys. Rev. A* 89, 022317 (2014), URL http://link.aps.org/doi/10.1103/PhysRevA.89.022317.

[5] P. Kómár, E.M. Kessler, M. Bishof, L. Jiang, A.S. Sørensen, J. Ye, and M.D. Lukin, "A quantum network of clocks," *Nat. Phys.* 10, 582–587 (2014).

[6] P.A. Knott, T.J. Proctor, A.J. Hayes, J.F. Ralph, P. Kok, and J.A. Dunningham, "Local versus global strategies in multiparameter estimation," *Phys. Rev. A* 94, 062312 (2016), URL https://link.aps.org/doi/10.1103/PhysRevA.94.062312.

[7] Z. Eldredge, M. Foss-Feig, J.A. Gross, S.L. Rolston, and A.V. Gorshkov, "Optimal and secure measurement protocols for quantum sensor networks," *Phys. Rev. A* 97, 042337 (2018), URL https://link.aps.org/doi/10.1103/PhysRevA.97.042337.

[8] J.W. Pan, D. Bouwmeester, H. Weinfurter, and A. Zeilinger, "Experimental Entanglement Swapping: Entangling Photons That Never Interacted," *Phys. Rev. Lett.* 80, 3891–3894 (1998), URL http://link.aps.org/doi/10.1103/PhysRevLett.80.3891.

[9] T. Yang, Q. Zhang, T.Y. Chen, S. Lu, J. Yin, J.W. Pan, Z.Y. Wei, J.R. Tian, and J. Zhang, "Experimental Synchronization of Independent Entangled Photon Sources," *Phys. Rev. Lett.* 96, 110501 (2006), URL https://link.aps.org/doi/10.1103/PhysRevLett.96.110501.

[10] R. Kaltenbaek, B. Blauensteiner, M. Żukowski, M. Aspelmeyer, and A. Zeilinger, "Experimental Interference of Independent Photons," *Phys. Rev. Lett.* 96, 240502 (2006), URL https://link.aps.org/doi/10.1103/PhysRevLett.96.240502.

[11] Q.C. Sun, Y.F. Jiang, Y.L. Mao, L.X. You, W. Zhang, W.J. Zhang, X. Jiang, T.Y. Chen, H. Li, Y.D. Huang, X.F. Chen, Z. Wang, J. Fan, Q. Zhang, and J.W. Pan, "Entanglement swapping over 100 km optical fiber with independent entangled photon-pair sources," *Optica* 4(10), 1214–1218 (2017), URL http://www.osapublishing.org/optica/abstract.cfm?URI=optica-4-10-1214.

[12] C.K. Hong, Z.Y. Ou, and L. Mandel, "Measurement of subpicosecond time intervals between two photons by interference," *Phys. Rev. Lett.* 59, 2044–2046 (1987), URL http://link.aps.org/doi/10.1103/PhysRevLett.59.2044.

[13] V. Giovannetti, L. Maccone, J.H. Shapiro, and F.N.C. Wong, "Generating Entangled Two-Photon States with Coincident Frequencies," *Phys. Rev. Lett.* 88, 183602 (2002), URL http://link.aps.org/doi/10.1103/PhysRevLett.88.183602.

[14] P.B. Dixon, J.H. Shapiro, and F.N.C. Wong, "Spectral engineering by Gaussian phase-matching for quantum photonics," *Opt. Express* 21(5), 5879–5890 (2013), URL http://www.opticsexpress.org/abstract.cfm?URI=oe-21-5-5879.

[15] R.B. Jin, M. Takeoka, U. Takagi, R. Shimizu, and M. Sasaki, "Highly efficient entanglement swapping and teleportation at telecom wavelength," *Sci. Rep.* 5, 9333 (2015).

[16] C. Chen, C. Bo, M.Y. Niu, F. Xu, Z. Zhang, J.H. Shapiro, and F.N.C. Wong, "Efficient generation and characterization of spectrally factorable biphotons," *Opt. Express* 25(7), 7300–7312 (2017), URL http://www.opticsexpress.org/abstract.cfm?URI=oe-25-7-7300.

[17] F. Graffitti, P. Barrow, M. Proietti, D. Kundys, and A. Fedrizzi, "Independent high-purity photons created in domain-engineered crystals," *Optica* 5(5), 514–517 (2018), URL http://www.osapublishing.org/optica/abstract.cfm?URI=optica-5-5-514.

[18] M.A. Broome, M.P. Almeida, A. Fedrizzi, and A.G. White, "Reducing multi-photon rates in pulsed down-conversion by temporal multiplexing," *Opt. Express* 19(23), 22698–22708 (2011), URL http://www.opticsexpress.org/abstract.cfm?URI=oe-19-23-22698.

[19] C. Greganti, P. Schiansky, I.A. Calafell, L.M. Procopio, L.A. Rozema, and P. Walther, "Tuning single-photon sources for telecom multi-photon experiments," *Opt. Express* 26(3), 3286–3302 (2018), URL http://www.opticsexpress.org/abstract.cfm?URI=oe-26-3-3286.

[20] M. Avenhaus, A. Eckstein, P.J. Mosley, and C. Silberhorn, "Fiber-assisted single-photon spectrograph," *Opt. Lett.* 34(18), 2873–2875 (2009), URL http://ol.osa.org/abstract.cfm?URI=ol-34-18-2873.

[21] M. Fiorentino and R.G. Beausoleil, "Compact sources of polarization-entangled photons," *Opt. Express* 16(24), 20149–20156 (2008), URL http://www.opticsexpress.org/abstract.cfm?URI=oe-16-24-20149.

[22] P.G. Evans, R.S. Bennink, W.P. Grice, T.S. Humble, and J. Schaake, "Bright Source of Spectrally Uncorrelated Polarization-Entangled Photons with Nearly Single-Mode Emission," *Phys. Rev. Lett.* 105, 253601 (2010), URL https://link.aps.org/doi/10.1103/PhysRevLett.105.253601.

[23] L.K. Shalm, E. Meyer-Scott, B.G. Christensen, P. Bierhorst, M.A. Wayne, M.J. Stevens, T. Gerrits, S. Glancy, D.R. Hamel, M.S. Allman, K.J. Coakley, S.D. Dyer, C. Hodge, A.E. Lita, V.B. Verma, C. Lambrocco, E. Tortorici, A.L. Migdall, Y. Zhang, D.R. Kumor, W.H. Farr, F. Marsili, M.D. Shaw, J.A. Stern, C. Abellán, W. Amaya, V. Pruneri, T. Jennewein, M.W. Mitchell, P.G. Kwiat, J.C. Bienfang, R.P. Mirin, E. Knill, and S.W. Nam, "Strong Loophole-Free Test of Local Realism," *Phys. Rev. Lett.* 115, 250402 (2015), URL http://link.aps.org/doi/10.1103/PhysRevLett.115.250402.

[24] A. Peres, "Separability Criterion for Density Matrices," *Phys. Rev. Lett.* 77, 1413–1415 (1996), URL https://link.aps.org/doi/10.1103/PhysRevLett.77.1413.

[25] O. Gühne and G. Tóth, "Entanglement detection," *Physics Reports* 474(1), 1–75 (2009), URL http://www.sciencedirect.com/science/article/pii/S0370157309000623.

This page intentionally left blank.